Intramolecular Charge-Transfer Dynamics in *p*-Dimethylaminobenzonitrile·Acetonitrile Clusters. A New Twist

Hiroyuki Saigusa,* Eijiro Iwase, and Masashi Nishimura

The Graduate School of Integrated Science, Yokohama City University, Yokohama 236-0027, Japan

Received: November 1, 2002; In Final Form: January 13, 2003

Excited-state dynamics of *p*-dimethylaminobenzonitrile (DMABN) complexed with acetonitrile solvent molecules, DMABN$(CH_3CN)_n$, have been investigated as a function of the cluster size using dispersed fluorescence spectroscopy implemented with time-of-flight mass analysis. No significant red shift in the fluorescence spectra is found to occur irrespective of the cluster size, when the clusters are excited in the vicinity of the S_1 electronic origin of the DMABN solute. As the excitation energy is increased, strongly red-shifted fluorescence which resembles the charge-transfer (CT) fluorescence in solution is detected for clusters of $n \geq 5$, while those of smaller sizes exhibit fragment fluorescence upon solvent evaporation. The size- and excitation-energy-dependent behavior suggests that the CT dynamics and subsequent relaxation in the jet-cooled clusters are controlled by microscopic hindrance of intramolecular structural changes due to solvent cage effects. Thus, the CT stabilization can be activated by increasing cluster internal temperatures and facilitating solvent reorganization.

Introduction

Since Lippert[1] discovered the dual fluorescence for DMABN in polar solvents, much work has been devoted to elucidating the origin of its red-shifted emission. While this excited-state behavior is explained qualitatively as intramolecular charge transfer (CT) accompanied by structural reorganization, the exact nature of the CT state is still under controversial discussion. The most prominent model, namely, the twisted intramolecular CT (TICT) model, has been proposed by Grabowski et al.,[2] which assumes that the dimethylamino group undergoes a twist of 90° with respect to the benzonitrile moiety in the CT state, allowing for charge separation. In the planar intramolecular CT (PICT) model developed by Zachariasse et al.,[3] it is postulated that the structure is nearly planar and the dimethylamino inversion motion is an important driving force for the CT reaction. Solvent effects on the CT stabilization in DMABN have also been investigated extensively, and the appearance of dual fluorescence is well-documented for sufficiently polar solvents.

It is perhaps most straightforward to learn the role of solvent in the CT dynamics by generating jet-cooled complexes of DMABN with solvent molecules and investigating them under collision-free conditions. The solvated clusters are expected to offer unique environments for studying specific solute−solvent interactions leading to the CT formation as a function of solvation number. So far, no evidence of dual-fluorescence behavior has been obtained for the bare DMABN molecule. Previous supersonic jet studies[4−7] showed red-shifted fluorescence behavior for clusters of methyl *p*-dimethylaminobenzoate with few solvent molecules. In this case, the lowest excited precursor state is considered to be of CT character since the energetically close lying S_2 state becomes accessible in small solvent clusters, presumably due to the stronger electron affinity of the methyl ester group.

Likewise, clusters of DMABN complexed with various solvent molecules have been investigated extensively using supersonic expansion techniques.[8−14] Kobayashi et al.[8] first reported fluorescence from 1:1 complexes of DMABN with water and trifluoromethane, but these complexes were found to exhibit no CT fluorescence. A similar result was obtained by Peng et al.[9] for the 1:1 complex with water. Gipson et al.[10] indicated that multiple solvation of DMABN with methanol results in a substantial decrease in the fluorescence quantum yield, suggesting the formation of a nonemissive CT state. Subsequently, Bernstein's group[11,12] measured $S_1 \leftarrow S_0$ spectra of DMABN complexes with polar solvents by means of resonance-enhanced two-photon ionization (R2PI) spectroscopy. For the 1:1 complex with acetonitrile, they found two structural isomers, one of which gives rise to fluorescence extending to longer than 400 nm.[12] Howell et al.[13] demonstrated dual-fluorescence behavior for DMABN complexes with various solvents and suggested that the long-wavelength emissions are associated with DMABN dimer or its solvated complexes, i.e., $(DMABN)_2(solvent)_n$. Analogous dual fluorescence was observed for DMABN complexes with acetonitrile by Krauss et al.[14] using dispersed fluorescence spectroscopy combined with mass analysis. Contrary to the result of Howell et al., they assigned the red-shifted component of the emission to CT fluorescence from the $(DMABN)_1(acetonitrile)_n$ clusters, and claimed that the CT formation requires a minimum of five acetonitrile molecules solvated with DMABN.

In this paper, the fluorescence behavior of DMABN$(CH_3CN)_n$ as a function of solvent size distribution is reexamined over a wide range of excitation energy. We have observed that these clusters exhibit red-shifted fluorescence assignable to CT formation when they are excited with a certain amount of excess energy. Furthermore, the minimum excess energy is found to depend strongly on the cluster size. The size- and excess-energy-dependent behavior is associated with CT formation and subsequent stabilization which are induced by increasing cluster internal temperatures. The result suggests that the CT dynamics

* To whom correspondence should be addressed. E-mail: saigusa@yokohama-cu.ac.jp.

10.1021/jp022362u CCC: $25.00
Published on Web 04/15/2003

in cold clusters is impeded by cluster rigidity, or solvent cage effects, and thus can be activated by solvent reorganization and relaxation.

Experimental Section

R2PI and dispersed fluorescence spectra were obtained by the experimental setup that has been described previously.[15,16] In the present case, DMABN was heated to 380 K, seeded into 4 atm of He, and expanded in a vacuum chamber through a 0.25 mm orifice of a pulsed valve. The nozzle temperature was kept at ~340 K to prevent the formation of homogeneous clusters of DMABN, since they are known to give rise to interfering fluorescence near 400 nm.[17] Acetonitrile was introduced by passing part of the helium carrier gas through a solvent reservoir and mixed with the sample vapor. The partial pressure of the solvent was carefully controlled by varying the reservoir temperature and the mixing ratio.

The resulting cluster beam was irradiated at 10 mm downstream with the frequency-doubled output of a YAG-pumped dye laser (Continuum PL8000/ND6000/UVT-1). Fluorescence spectra were recorded by a PMT tube through a 0.32 m monochromator (Jobin-Yvon HR320 with a 1200 lines/mm grating blazed at 330 nm) at a spectral resolution of 5 nm. The system response function was checked by measuring fluorescence from DMABN in acetonitrile solution with the same excitation and detection system. The bulk spectrum was then compared with a quantum-corrected fluorescence spectrum of the same sample with a spectrofluorometer for correction. The corrected spectrum was essentially identical to that reported by Rettig and Zietz.[18]

For recording cluster size distribution, the molecular beam was skimmed and introduced in a second differentially pumped chamber where it was intersected by a portion of the UV laser beam. The cluster cations were mass analyzed by a Wiley−McLaren-type linear time-of-flight mass spectrometer and detected with a microchannel plate. The resulting mass spectrum enabled us to obtain information on the cluster size distribution in a nozzle expansion and identify the species that contributes the corresponding dispersed fluorescence spectrum.

Results and Discussion

The R2PI spectra of DMABN$(CH_3CN)_n$ for $n = 0-10$ in the energy region of the monomer S_1 origin at 32244 cm^{-1} (bottom spectrum) are shown in Figure 1. The $n = 1$ cluster gives sharp absorption features and underlying broad bands, which can be assigned to two different structural isomers on the basis of the result by Shang and Bernstein.[12] The spectra for $n \geq 2$ exhibit no well-resolved features, indicating that size-selective excitation is essentially impossible in this energy region.

Figure 2 illustrates the dispersed fluorescence spectra and corresponding mass spectra taken under the same experimental conditions as employed for the emission spectra. In both cases, excitation was performed at 306 nm (~435 cm^{-1} above the monomer origin, as indicated in Figure 1), where no prominent spectral features of the monomer or clusters are apparent. As the cluster size distribution is increased toward larger clusters, the emission maximum shifts to the red of the excitation. In the case of the largest cluster distribution H, where $n = 10-20$ clusters are discernible in the corresponding mass spectrum, its emission spectrum appears with an intensity maximum at ~350 nm. This emission is red-shifted only by ~20 nm with respect to the smallest cluster case (spectrum A). Further increase in the cluster size distribution shows that a terminal red shift of ~20 nm is nearly attained for $n > 10$. It is therefore concluded that the fluorescence spectra do not converge to that of the CT fluorescence in room-temperature solution, which peaks at ~470 nm.

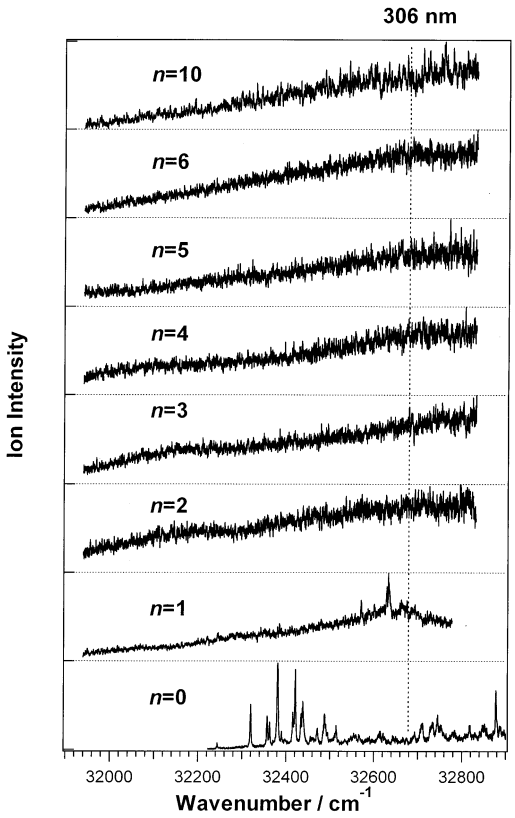

Figure 1. R2PI spectra of DMABN$(CH_3CN)_n$ for $n = 0-10$ in the energy region of the monomer S_1 origin at 32244 cm^{-1}. The dotted line corresponds to the excitation wavelength of 306 nm used to record the fluorescence spectra in Figure 2.

A careful examination of the fluorescence spectra B and C reveals that there is a clear shift in their maxima. The corresponding mass spectra indicate that $n = 3-5$ clusters are more abundant in spectrum C. The relatively small, albeit very distinct, red shift of fluorescence at $n = 3-5$ agrees with the result for DMABN$(water)_n$ clusters. In the case of the water clusters, cluster-selective excitation is possible for $n \leq 3$ due to the discrete nature of their absorption spectra, thus permitting quantitative comparison of fluorescence maxima.[19] The result indicates that CT stabilization occurs weakly at $n = 3$, although its stability is significantly less than in solution. In both water and acetonitrile clusters, a further red shift is seen for a larger cluster distribution, but only slightly with respect to the spectra of $n \leq 3$. These observations suggest that the CT dynamics and subsequent relaxation in both clusters are substantially inhibited as a result of solvent cage effects, and the observed fluorescence may be assigned as arising from an *unrelaxed* state of CT character which correlates with the second excited state S_2, as discussed below.

In contrast to our observation, Howell et al.[13] reported dual fluorescence in DMABN·acetonitrile clusters. They assigned the redder component of the fluorescence centered at 414 nm as arising from a DMABN dimer or its solvated clusters, on the basis of the temperature dependence of its intensity. Similar greatly red-shifted fluorescence was observed at 425 nm by Krauss et al.[14] for a cluster size distribution where clusters of $n \geq 5$ are noticeable. The red-shifted component was obtained through excitation at 306.24 nm (corresponding to the most

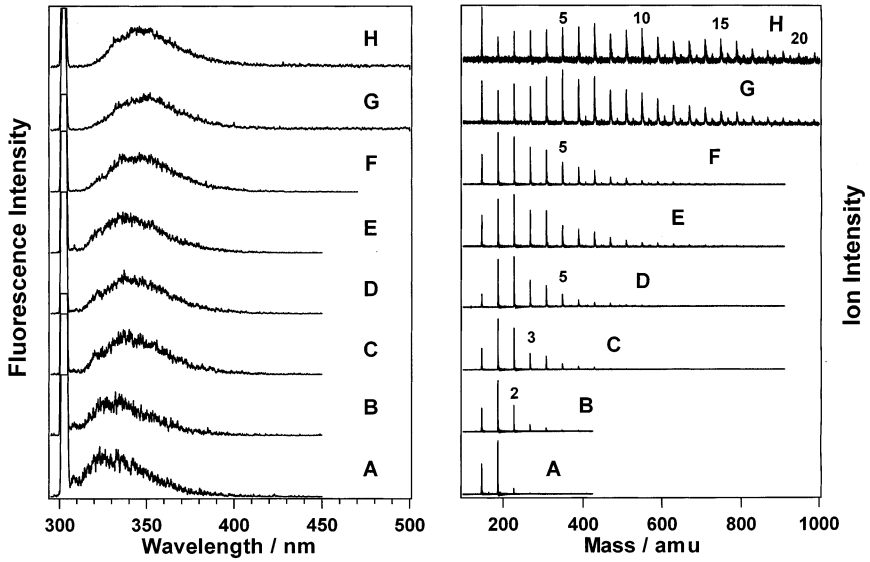

Figure 2. Fluorescence spectra of DMABN$(CH_3CN)_n$ clusters for different size distributions. The corresponding mass spectra taken under the same expansion conditions are shown in the right panel. In all cases, the excitation wavelength is 306 nm. The leftmost peak in each fluorescence spectrum is attributed to scattered laser light. The spectral resolution is 5 nm. The mass peaks corresponding to clusters of $n \leq 3$ in the mass spectra G and H are predominantly due to fragmentation upon ionization.

prominent feature of the $n = 1$ cluster in Figure 1), and attributed to CT fluorescence from clusters of $n \geq 5$. Although we suggest that clusters involving a DMABN dimer are responsible for the appearance of the dual fluorescence at this excitation energy, a more detailed investigation is definitely needed for explaining the apparently different observations.

On the basis of the lack of any strongly red-shifted fluorescence even for the largest observed clusters ($n > 20$) in our study, we assume that the DMABN solute embedded in an acetonitrile cage can undergo few conformational changes as a result of barriers along the CT stabilization coordinate. This behavior is presumably due to the low internal temperatures associated with the clusters generated using jet expansions. It is also consistent with the result of Suzuka et al.[20] obtained for DMABN in an acetonitrile matrix, which indicates that its CT emission is suppressed and only the phosphorescence of DMABN appears below 195 K. The importance of such solvent cage effects was put forward previously by Knochenmuss and Leutwyler[21] for the excited-state proton transfer (ESPT) dynamics in 1-naphthol·water clusters. They suggested that the extent of ESPT occurring in these clusters is largely controlled by solvent rigidity and thus different from the behavior in room-temperature bulk water. Furthermore, Knochenmuss and Smith[22] demonstrated that the red shift of ESPT fluorescence in these clusters becomes more extensive as the cluster internal temperature is increased, from which the role of solvent relaxation in ESPT was inferred.

It is usually difficult to generate such solvent clusters with a desired size distribution over a relevant temperature range and probe their dynamics as a function of cluster internal energy. When expansion conditions and thus effective temperatures are changed, cluster distributions change as well. In the present study, we attempt to measure the CT dynamics in DMABN-$(CH_3CN)_n$ clusters over a wide range of excitation energy without such complications. Figure 3 shows the fluorescence spectrum obtained following excitation at 275 nm for the cluster distribution E shown in Figure 2. As compared with that recorded at 306 nm, a new red-shifted emission is clearly apparent around 450 nm, which matches well the CT fluorescence observed in acetonitrile solution at 300 K (lower spectrum). This excitation corresponds to an excess energy of

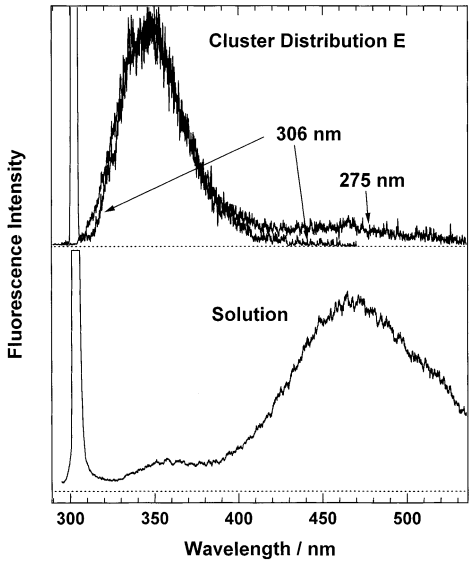

Figure 3. Fluorescence spectra obtained following excitations at 306 and 275 nm for the cluster size distribution E in Figure 2. The fluorescence spectrum of DMABN in acetonitrile solution (10^{-5} M) at 300 K is shown in the lower panel, which is obtained following excitation at 306 nm and by measuring with the same detection apparatus as used for taking the upper spectra. All spectra are corrected for the response of the entire detection system.

4100 cm^{-1} from the monomer origin. The corresponding cluster distribution, which is obtained at 306 nm, indicates that medium-sized clusters of $n = 5-10$ are abundant. It is also notable that the 275 nm spectrum exhibits additional fluorescence near 320 nm compared to the 306 nm spectrum. The blue-shifted emission can be attributed to fragment fluorescence from smaller clusters which are produced upon evaporation of solvent molecule(s).

The red-shifted component of the emission, termed *relaxed* CT fluorescence, is found to grow in relative intensity with excess energy, depending crucially on the cluster size distribution. Figure 4 demonstrates such behavior for three different cluster size distributions (C, E, and G in Figure 2). The excitation wavelengths are 290 and 280 nm, which correspond to excess energies of 2225 and 3457 cm^{-1}, respectively. The emission spectra for the small-sized clusters C, where clusters

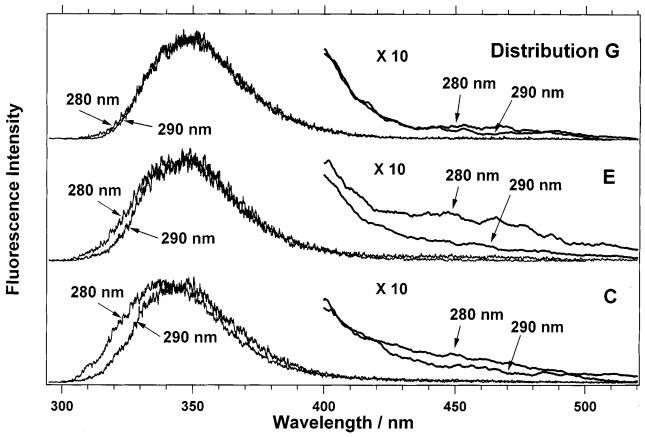

Figure 4. Fluorescence spectra (uncorrected for the detection response) obtained following excitations at 290 and 280 nm for the different cluster size distributions C, E, and G in Figure 2. The corresponding excess energies are 2225 and 3457 cm^{-1}, respectively, above the monomer S_1 origin. Also shown are the red portions of the spectra with an expanded scale.

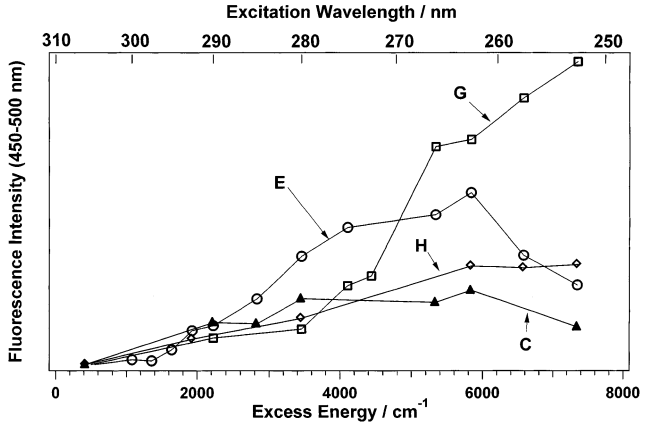

Figure 5. Intensity ratios of the red portion of the fluorescence spectrum to the band maximum as a function of excess energy. The red-shifted fluorescence intensity is calculated by integrating the fluorescence in the wavelength range between 450 and 500 nm. The corresponding size distributions (C, E, G, and H) are depicted in Figure 2. The excess energy is relative to the monomer S_1 origin.

of $n < 5$ dominate, show weak CT fluorescence around 450 nm. Its intensity increases slightly as the excitation wavelength is shifted to 280 nm. More importantly, a spectral shoulder develops at the blue side of the 290 nm fluorescence. As described above, this behavior is associated with fragmentation for small clusters of $n < 5$. For the medium-sized cluster distribution E, the relative strength of the CT fluorescence substantially increases in going from 290 to 280 nm while that of the fragment fluorescence is less than in spectra C. As the cluster size distribution is shifted further to larger sizes (spectra G), little red-shifted fluorescence is observed in this excitation wavelength range, which predicts that more activation energy is required for CT stabilization in larger clusters of $n \geq 10$.

The data presented above show that the excess energy deposited on the solute has a significant effect on the appearance of red-shifted fluorescence in DMABN$(CH_3CN)_n$ clusters. The size and excess energy dependence of the relaxed CT fluorescence intensity is summarized in Figure 5. The threshold excess energy for the CT stabilization appears to be dependent strongly on the cluster size distribution. For the moderate-sized clusters $n = 5-10$ (spectrum E), it is estimated to be in the range 2500−3000 cm^{-1}. A further increase in the excess energy above 6000 cm^{-1} leads to a decrease in the CT fluorescence intensity, consistent with the occurrence of cluster fragmentation. A more pronounced threshold is seen at ∼4000 cm^{-1} for the larger clusters (spectrum G). As the clusters increase further in size (spectrum H), threshold behavior is yet to be observed. This excess-energy-dependent behavior of CT activation cannot be explained by an assertion that the dynamics would be promoted via direct excitation into the relaxed CT state without solvent reorganization. If such direct CT excitation prevailed, lower CT threshold energies should be observed for larger clusters.

These observations suggest that the major factor controlling the extent of CT stabilization is the balance of the excess energy and cluster size. This is consistent with the cluster-rigidity scenario that the dynamics in the cold clusters is kinetically limited by a solvent cage. When an excess amount of energy is deposited on the solute, it will flow rapidly into solute−solvent modes, thereby enabling reorientation of the solvent molecules in the proximity of the solute. This in turn facilitates geometrical changes of the solute, leading to CT, while evaporating solvent molecule(s) which are presumably located on the exterior of the cluster. At a given excess energy, only a certain size range of the clusters is expected to undergo CT formation via such solvent relaxation. Other smaller clusters dissociate to produce less red-shifted fluorescence, while no dynamics can be activated in larger clusters with this excess energy. The size-dependent fluorescence behavior accounts for the relatively weak CT fluorescence in the 275 nm spectrum of Figure 3 compared to that in the bulk spectrum.

On the basis of these considerations, an inference is made that the CT stabilization is accompanied by substantial changes in the conformation of the solute such as those implicated in the TICT model,[2] i.e., twisting of the dimethylamino group with respect to the benzonitrile moiety. However, an electronic factor should also be taken into account for explaining the CT nature of these solvated clusters on the basis of such a steric-rigidity picture. In contrast, little relaxed CT fluorescence is observed in DMABN·water clusters when excited over the same excess energy range.[19] The lack of significant CT stabilization in water clusters can be associated with solvent reorganization which must involve breaking of hydrogen bonds. The structural-rigidity scenario suggests that a more excess energy is required for activation of CT in water clusters. Another possible factor for the difference between the water and acetonitrile clusters is local solvent structure. In the DMABN·water clusters, the solvent molecules tend to cluster together and solvate to the solute. They are expected to dissociate together upon excitation to produce smaller clusters having a few water molecules, thus explaining the absence of CT stabilization.

In conclusion, we have observed that the extent of CT stabilization in DMABN$(CH_3CN)_n$ clusters is much less than in bulk solution and does not converge to the bulk limit as the cluster size is increased. This observation suggests that the CT stabilization in larger clusters is slowed or impeded by solvent cage effects associated with the low cluster temperature. A bulklike CT fluorescence is observed for larger clusters when they are excited at higher energies. The minimum excess energy required for the CT activation appears to be strongly dependent on the cluster size. This dynamical behavior is associated with solvent reorganization and relaxation which enable conformational changes of the solute, leading to CT. On the basis of the present observation, the cluster CT dynamics is expected to be gradually extrapolated to that occurring in bulk solution upon increasing the cluster temperatures and facilitating solvent reorganization.

Acknowledgment. We are grateful to Professor I. Suzuka for communicating his results prior to publication. This work was supported in part by the Sumitomo Foundation.

References and Notes

(1) Lippert, E.; Lüder, W.; Boos, H. In *Advances in Molecular Spectroscopy*; Mangini, A., Ed.; Pergamon: Oxford, 1962; p 443.
(2) Rotkiewicz, K.; Grellman, K. H.; Grabowski, Z. R. *Chem. Phys. Lett.* **1973**, *19*, 315.
(3) Zachariasse, K. A.; von der Haar, Th.; Hebeker, A.; Leinhos, U.; Kühnle, W. *Pure Appl. Chem.* **1993**, *65*, 1745.
(4) Weersink, R. A.; Wallace, S. C. *J. Phys. Chem.* **1994**, *98*, 10710.
(5) Dedonder-Lardeux, C.; Jouvet, C.; Martrenchard, S.; Solgardi, D. McCombie, J.; Howells, B. D.; Palmer, T. F.; Subaric-Leitis, A.; Monte, C.; Rettig, W.; Zimmermann, P. *Chem Phys.* **1995**, *191*, 271.
(6) Grégoire, G.; Dimicoli, I.; Mons, M.; Dedonder-Lardeux, C.; Jouvet, C.; Martrenchard, S.; Solgardi, D. *J. Phys. Chem. A* **1998**, *102*, 7896.
(7) Krauss, O.; Brutschy, B. *Chem. Phys. Lett.* **2001**, *350*, 427.
(8) Kobayashi, T.; Futakami, M.; Kajimoto, O. *Chem. Phys. Lett.* **1986**, *130*, 63.
(9) Peng, L. W.; Dantus, M.; Zewail, A. H.; Kemnitz, K.; Hicks, M.; Eisental, K. B. *J. Phys. Chem.* **1987**, *91*, 6162.
(10) Gibson, E. M.; Jones, A. C.; Phillips, D. *Chem. Phys. Lett.* **1987**, *136*, 454.
(11) Grassian, V. H.; Warren, J. A.; Bernstein, E. R.; Secor, H. V. *J. Chem. Phys.* **1989**, *90*, 3994.
(12) Shang, Q.; Bernstein, E. R. *J. Chem. Phys.* **1992**, *97*, 60.
(13) Howell, R.; Phillips, D.; Petek, H.; Yoshihara, K. *Chem. Phys.* **1994**, *188*, 303.
(14) Krauss, O.; Lommatzsch, U.; Lahmann, C.; Brutschy, B.; Rettig, W.; Herbich, J. *Phys. Chem. Chem. Phys.* **2001**, *3*, 74.
(15) Hirata, T.; Ikeda, H.; Saigusa, H. *J. Phys. Chem. A* **1999**, *103*, 1014.
(16) Saigusa, H.; Morohoshi, M.; Tsuchiya, S. *J. Phys. Chem. A* **2001**, *105*, 7334.
(17) Lommatzsch, U.; Gerlach, A.; Lahmann, C.; Brutschy, B. *J. Phys. Chem. A* **1998**, *102*, 6421.
(18) Rettig, W.; Zietz, B. *Chem. Phys. Lett.* **2000**, *317*, 187.
(19) Saigusa, H.; Iwase, E.; Nishimura, M. *J. Phys. Chem. A*, in press.
(20) Suzuka, I. Private communication.
(21) Knochenmuss, R.; Leutwyler, S. *J. Chem. Phys.* **1989**, *91*, 1268.
(22) Knochenmuss, R.; Smith. D. E. *J. Chem. Phys.* **1994**, *101*, 7327.